Deep Learning-based receiver for Uplink in LoRa Networks with Sigfox Interference

Angesom Ataklity Tesfay[1,2], Eric Pierre Simon[1], Sofiane Kharbech[2], and Laurent Clavier[1,2]
[1]Univ. Lille, CNRS, UMR 8520 - IEMN, F-59000, Lille, France (e-mail: firstname.name@univ-lille.fr)
[2]IMT Nord Europe, France (e-mail: firstname.name@imt-nord-europe.fr)

***Abstract*—The Internet of Things faces a significant scaling issue due to the rapid growth of the number of devices and asynchronous communications. Different technologies in the license-free industrial, scientific, and medical (ISM) band have been widely deployed to fill this gap. LoRa and Sigfox are the most common. Many devices can use the ISM band if they obey the regulations and cope with internal and external interference. However, when there is massive connectivity, the effect of the inter and intra-network interference between multiple networks is significant. This study uses a deep learning-based technique to decode signals and deal with the interference in the uplink of a LoRa network. Two classification-based symbol detection methods are proposed using a deep feedforward neural network (DFNN) and a convolutional neural network (CNN). The proposed receivers can decode the signals of a selected user when many LoRa users transmit simultaneously using the same spreading factor over the same frequency band (intra-spreading factor interference), and multiple Sigfox users interfere (inter-network interference). Simulation results show that both receivers outperform the conventional LoRa receiver in the presence of interference. For a target symbol error rate (SER) of 10^{-3}, the proposed DFNN and CNN-based receivers attain around 2 dB and 3.5 dB gain, respectively.**

***Index Terms*—LoRa, IoT, deep learning, neural networks, capture effect.**

I. Introduction

The Internet of Things (IoT) networks have been getting more and more interest recently, and long-range, low-power communication networks are mainly implemented. These networks enable connectivity for many devices with a single base station by sacrificing throughput. Contrary to cellular networks, IoT networks are also widely deployed in the license-free industrial, scientific, and medical (ISM) frequency band. LoRa and Sigfox are the most common IoT connectivity technologies deployed in these bands.

LoRa is based on a chirp spread spectrum (CSS) modulation technique, and it allows quasi-orthogonal transmissions using different spreading factors (SF) and bandwidth settings. However, collisions occur at the receiver when two or more devices simultaneously transmit with the same SF on the same frequency band [1], generally resulting in packet loss. A single packet can be correctly decoded despite the collision using the receiver's capture effect phenomenon. The capture effect can be achieved when the desired signal is stronger than the interfering one. On the other hand, Sigfox is an ultra-narrowband (UNB) technology using differential binary phase-shift keying (DBPSK) with a 100 Hz channel. The license-free ISM band allows many different devices to access the spectrum as long as they obey the regulations and deal with internal and external interference. Most of the publications assume that the interference between multiple networks for long-range communication can be ignored, as the number of signals that each device transmits is typically low. However, inter and intra-cell interference studies in [2], [3] show that interference does matter when there is massive connectivity of devices. In this paper, we will focus on the impact of interference on a LoRa user from other LoRa interfering user and Sigfox user.

Most of the works deal with intra-technology interference. In [4] an interleaved chirp spreading (ICS) modulation scheme is implemented to cope with co-SF interference in LoRa. However, the proposed modulation scheme is not directly backward compatible with the LoRaWAN standard, and interference from other networks was not considered. In [5], a serial interference cancellation (SIC) scheme was used to decode the strongest user first, then suppress it, and the second strongest can be decoded afterward. Some works in the literature use deep learning approaches for IoT networks [6]–[8], but not in the context of signal detection. In [9], we proposed two signal detection techniques for the uplink LoRa based on deep learning. However, only the co-SF interference is considered, and the neural networks' hyperparameters are not optimized.

In this paper, we propose deep learning-based signal detection approaches for the uplink in LoRa networks which significantly improve the receiver's detection capability in the presence of interference from LoRa (co-SF) and Sigfox users. To our knowledge, there are no works that study LoRa signal detection and deal with both LoRa and Sigfox interference.

The contributions of this paper are summarized as follows: (i) We design two deep learning-based receivers for signal detection in LoRa networks uplink communication, which deals with symbol detection with a classification approach. These receivers can deal with interference coming from other LoRa as well as Sigfox users, and both significantly improve the capture effect compared to the classical LoRa receiver; (ii) the setup of a Bayesian-optimized complete decoding scheme; and (iii) maintaining a low complexity.

The paper is organized as follows. The system model is described in the following section. Section III presents the two proposed deep learning-based receivers. The simulation results and discussions are shown in Section IV. In Section V the conclusions are drawn.

II. System Model

A. LoRa

Each symbol is represented by SF bits with $M = 2^{\text{SF}}$ possible symbols, and the SF spans from 7 to 12. The symbol duration is given by $T_s = MT$, where the sampling period is $T = \frac{1}{B}$ and B denotes the signal bandwidth. A chirp is used to represent each LoRa symbol, and it comprises a linear frequency shift over the symbol duration T_s. It is generated from a raw chirp $s(t)$, with the instantaneous frequency $\frac{B}{T_s}t$, giving the base-band expression:

$$s(t) = e^{\jmath 2\pi \frac{B}{2T_s}t^2} \quad t \in \left[-\frac{T_s}{2}, \frac{T_s}{2}\right]. \tag{1}$$

Let P be the total number of LoRa symbols in one packet. The jth user transmits the symbol $m_j^{(p)} \in \{0, ..., M-1\}$ at time pT_s $(p = 0, \cdots, P-1)$. The information is encoded by performing a cyclic shift of the raw chirp by $\delta_j^{(p)} = m_j^{(p)}T$, as indicated in Fig. 1. Hence, the coded chirp is:

$$s_j^{(p)}(t) = \begin{cases} e^{\jmath 2\pi\left[\frac{B}{2T_s}t^2 + \frac{m_j^{(p)}}{T_s}t\right]}, & t \in \left[-\frac{T_s}{2}, \frac{T_s}{2} - \delta_j^{(p)}\right), \\ e^{\jmath 2\pi\left[\frac{B}{2T_s}t^2 + \left(\frac{m_j^{(p)}}{T_s} - B\right)t\right]} & t \in \left[\frac{T_s}{2} - \delta_j^{(p)}, \frac{T_s}{2}\right]. \end{cases}$$

The jth user transmits the signal $s_j(t) = \sum_{p=0}^{P-1} s_j^{(p)}(t - pT_s)$. A preamble of raw chirps is prepended to the transmitted LoRa packet.

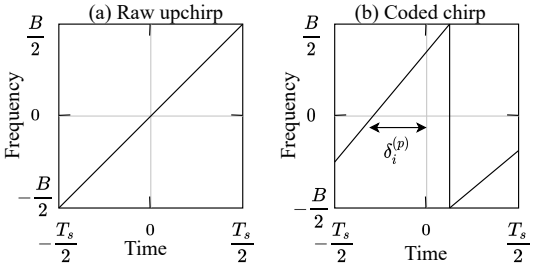

Fig. 1: (a) Raw chirp (b) Coded chirp associated with $m_j^{(p)}$.

B. Sigfox

The symbols are modulated using DBPSK modulation scheme at a very low rate $R = 100$ bps. Thus, the transmitted signal occupies a band of approximately $W_s = 100$ Hz. Sigfox devices employ a Random Frequency and Time Division Multiple Access to transmit their signals. The frequency hopping is done inside a bandwidth $B \gg W_s$, which ensures channel diversity. The expression for a symbol (p) transmitted by the Sigfox user l is:

$$x_l^{(p)}(t) = A^{(p)}g(t - pT_l)e^{2\imath\pi f_b t} \tag{2}$$

where $T_l = \frac{1}{R}$ is the symbol period, $A^{(p)}$ is the DBPSK symbol transmitted at time pT_l, f_b is the carrier frequency shift, and $g(t)$ is the pulse shaping filter with bandwidth of W_s.

We considered a circle with a radius of r_{max} and a gateway located at the center with a user-free area around the gateway with a radius of r_{min}. Assume N_{LoRa} and N_{sigfox} are the numbers of interfering LoRa and Sigfox users, respectively, randomly selected from a Poisson distribution with parameter λ. The 2D coordinates of the N_{LoRa} and N_{sigfox} interfering users are uniformly distributed while considering only positions within the disc defined by r_{max} and r_{min}. As the different devices operate autonomously, the transmission between nodes is asynchronous. The correlation between the received signal and the preamble is used for synchronization at the receiver. The received signal corresponding to symbol p sampled at $t = nT - pT_s$, $n = -\frac{M}{2}, \cdots, \frac{M}{2} - 1$ synchronized for the LoRa user j is:

$$r^{(p)}[n] = h_j s_j^{(p)}[n] + \text{LoRa}^{(\text{interference})} + \text{Sigfox}^{(\text{interference})} + w^{(p)}[n], \tag{3}$$

where $s_j^{(p)}[n] = s_j^{(p)}(nT)$, $w^{(p)}[n] \sim \mathcal{CN}(0, \sigma^2)$ is a circularly symmetrical complex Gaussian noise and h_j is the channel coefficients for LoRa users j.

Figure 2 illustrates the collision between the pth symbol of the selected LoRa user j, consecutive symbols of interfering LoRa, and Sigfox users.

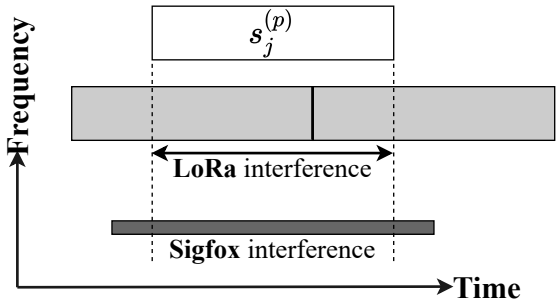

Fig. 2: Collision between a symbol of desired user and two consecutive symbols of the interfering user.

In the classical LoRa receiver, the demodulation process starts by multiplying the samples of the received signal $r^{(p)}[n]$ by the conjugate of the raw chirp, resulting $y^{(p)}[n] = r^{(p)}[n]s^*[n]$, where $s^*[n] = s^*(nT)$. Then, a Fast Fourier Transform (FFT) is applied:

$$Y^{(p)}[k] = \sum_{n=-M/2}^{M/2} y^{(p)}[n]\, e^{-2\imath\pi\frac{nk}{M}},\ k = 0, \ldots, M-1. \tag{4}$$

Then the symbol $m_j^{(p)}$ is determined by taking the frequency index where the modulus of (4) is maximum. However, it is not able to handle when collisions between multiple users occur.

III. Proposed Deep Learning-based receiver

This section presents the proposed Deep Feedforward Neural Network (DFNN) and Convolutional Neural Network (CNN)-based receivers.

A. Deep Feedforward Neural Network-based receiver

The receiver is based on a DFNN architecture with a series of fully connected layers, followed by Batch normalization (BN) to prevent overfitting, as shown in Fig. 3. The number and the size of each fully connected layer are determined through Bayesian optimization. The input is the vertical concatenation of the real and imaginary part of the de-chirped received samples after the FFT (4), resulting in $2M$ input nodes. The transmitted symbols are the output, yielding M output nodes. The ReLU function is applied as the activation function and the softmax function is used for classification in the output layer.

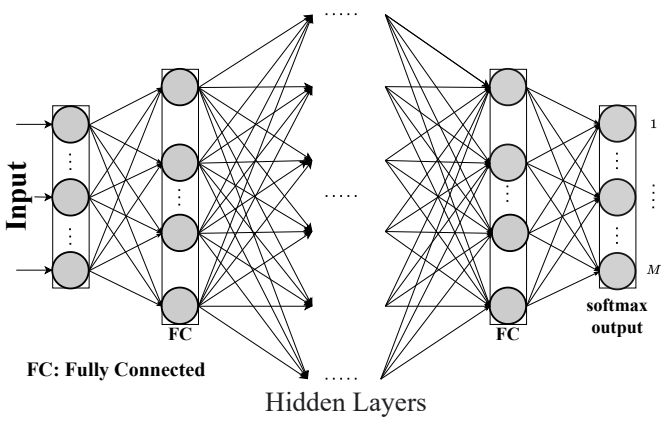

Fig. 3: Deep Feedforward Neural Network architecture.

The DFNN is trained to minimize the cross-entropy loss between the detected and the transmitted symbols.

B. Convolutional Neural Network-based receiver

CNN is based on convolutional processes inside the convolutional layers. The input for this architecture is illustrated as an $M \times M$ binary image of the modulus plots of (4), as shown in Fig. 4. The M nodes at the output layer are associated with the M transmitted symbols. As indicated in Fig. 5, the CNN structure comprises several convolutional layers, a pooling layer, and a set of fully connected layers. Bayesian optimization is applied to set parameters such as the number of convolutional and fully connected layers, the number of filters and their sizes, and the size of each fully connected layer. The ReLU function is implemented as the activation function, similar to the DFNN, and batch normalization is applied. The softmax function is used to classify and map the symbols in the output layer. The CNN is trained to minimize the loss in cross-entropy between the output and transmitted symbols.

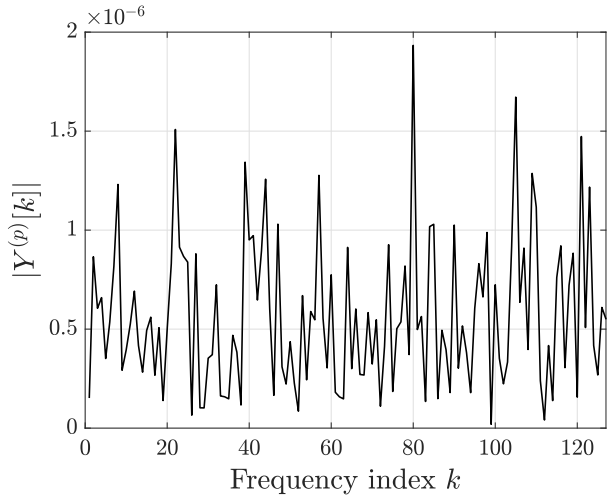

Fig. 4: Plot of $|Y^{(p)}[k]|$ ($k = 0, \cdots, M-1$) for a symbol of $m^{(p)} = 80$ with SNR $= -10$ dB and SF $= 7$.

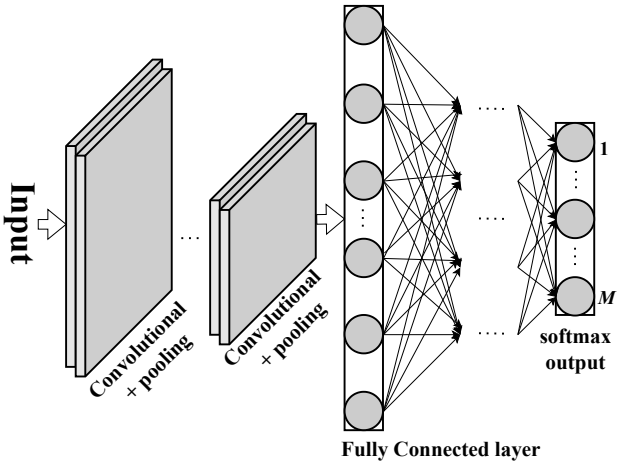

Fig. 5: Convolutional Neural Network architecture.

IV. Simulation Results

This section presents the performance evaluation of the proposed DFNN and CNN-based receivers. For each signal-to-noise ratio (SNR) value, the training is done offline using training data generated from the simulation. For the LoRa transmission, we considered a bandwidth $B = 250$ kHz, with SF $= 7$, giving $M = 128$. The r_{max} and r_{min} are set to 1 km and 20 m, respectively. N_{LoRa} and N_{sigfox} are drawn from a Poisson distribution as described in section II, with parameter $\lambda = 0.25$, 0.5, 0.7, and 1. The hyperparameters of DFNN and CNN are tuned through a Bayesian hyperparameter optimization process. The number of convolutional layers (nCL), fully connected layers (nFC), filters (nf); the size of the filters (sf) and fully connected layers (sFC). The Bayesian optimization step is performed separately for each value of λ. Additionally, initial experimental tryouts indicated that running that step for SNR$= -8$ dB is sufficient to have a network structure that could be generalized for the other considered SNR values.

Tables I and II list the optimized structure for both DFNN and CNN parts, where the number of the corresponding layer is indicated by the subscripts. The number of filters of the CNN and their sizes augments with the severity of the interference. Similarly, the number of hidden layers in the DFNN part and their corresponding size increases as the number of interference increases. It should be noted that the size of the last FC layer is fixed to M as illustrated in Fig.

TABLE I: Bayesian-optimized hyperparameters of the DFNN as a function of λ.

λ	nFC	sFC_1	sFC_2	sFC_3	sFC_4
0.25	4	313	224	188	128
0.7	4	562	307	230	128
1	4	759	428	295	128

5. In the literature, there are no works that investigate LoRa signal detection by dealing with LoRa and Sigfox interference. However, the work in [9] is the closest in the context of deep learning-based. Therefore, we compared the proposed receivers with the receivers in [9] and the classical LoRa receiver using the symbol error rate (SER) as the function of SNR.

TABLE II: Bayesian-optimized hyperparameters of the CNN as a function of λ.

λ	nCL	nf_1	nf_2	sf_1	sf_2	nFC	sFC_1	sFC_2
0.25	2	32	84	2	4	2	251	128
0.7	2	53	96	3	8	2	379	128
1	2	76	120	6	8	2	453	128

In the following, first, we fixed the SNR value to evaluate the performance of the receivers as a function of N_{LoRa} interfering users. Then we present results where N_{LoRa} and N_{sigfox} are random variables.

A. Performance under LoRa Interference

Figure 6 illustrates the SER performance of decoding a selected user as a function of the number of interfering users N_{LoRa} for the SNR $= -7$. The proposed receivers can decode the signal of the selected user in the presence of $N_{\text{LoRa}} = 3$ and 5 interfering users (Co-SF) for a target SER of 10^{-3} and 10^{-2}, respectively. Moreover, with the presence of more interfering LoRa users, the performance of the classical LoRa receiver degrades significantly.

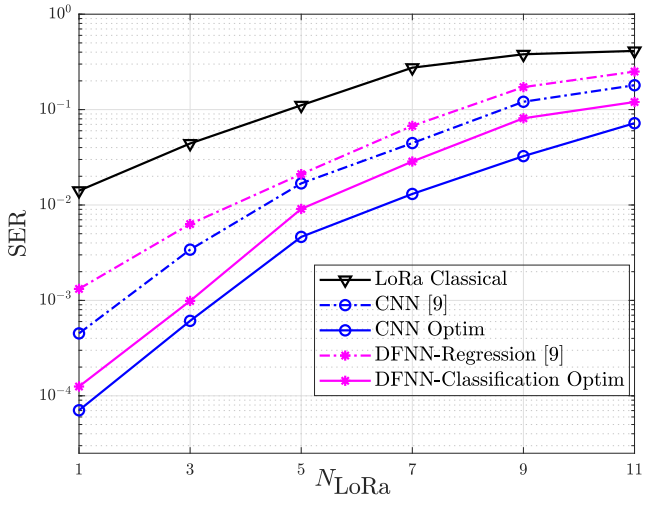

Fig. 6: SER as a function of number of interfering users N_{LoRa} for different detection approaches: *classical receiver*, *DFNN-based* [9], *CNN-based* [9], and the proposed receivers.

B. Performance under LoRa and Sigfox Interference

As explained in section II, in a given time interval the total number of interfering users N_{LoRa} and N_{sigfox} are drawn from a Poisson distribution, with $\lambda = 0.25$, 0.5, 0.7, and 1. The training and test are carried out for each pair of SNR and λ. Figure 7 shows the simulation results of the proposed receivers compared with the receivers in [9] and the classical LoRa receiver. It is illustrated that the proposed receivers outperform the deep learning-based receivers in [9] and the classical LoRa receiver for different λ.

In the case of fewer interfering users ($\lambda = 0.25$ and 0.5), the proposed DFNN and CNN-based receivers are more efficient than the receivers in [9] with 1.5 dB and 3 dB gain, respectively, for a target SER of 10^{-3} (cf. Figs. 7a and 7b). For the higher number of interfering users ($\lambda = 0.7$ and 1) and the same target SER of 10^{-3}, the proposed DFNN and CNN-based receivers obtain around 2 dB and 3.5 dB, respectively (cf. Fig. 7c and 7d).

C. Complexity Analysis

The classical LoRa receiver's computational complexity order is $\mathcal{O}(M \log(M))$ [10]. The complexity of the DFNN-based receiver is estimated to be $\mathcal{O}(M^2)$. For the CNN-based receiver, the computational complexity remains in the order of $\mathcal{O}(M^2)$, which is driven from [11]. The computational complexity of the proposed receivers remains in the same order as the receivers in [9], which is $\mathcal{O}(M^2)$.

The complexity would be high for the LoRa end device; however, it is acceptable in the access point where the signal detection is performed, and the cost and computing capacity are significantly higher.

V. Conclusion

This paper studied optimized deep learning-based techniques for uplink LoRa networks that can decode the signals of a selected user while considering interfering Sigfox users and LoRa interfering users, which transmit simultaneously using the same SF over the same frequency channel. The simulation results show that the two proposed DFNN-based and CNN-based receivers outperform the receivers in [9] and the classical LoRa receiver in the presence of interference. In the presence of higher interference and for a target SER of 10^{-3}, the proposed DFNN and CNN-based receivers attain around 2 dB and 3.5 dB gain, respectively (cf. Fig. 7c and 7d). The computational complexity order of the proposed receivers is kept efficient while improving the performance.

Deep learning-based techniques appear to be an attractive solution for addressing the issue of interference in IoT networks caused by the exponential growth of connected devices in the future. Additionally, for SNR $= -7$ dB, we have shown that the proposed receivers can decode the signal of the selected user in the presence of $N_{\text{LoRa}} = 3$ and 5 interfering users for a target SER of 10^{-3} and 10^{-2}, respectively.

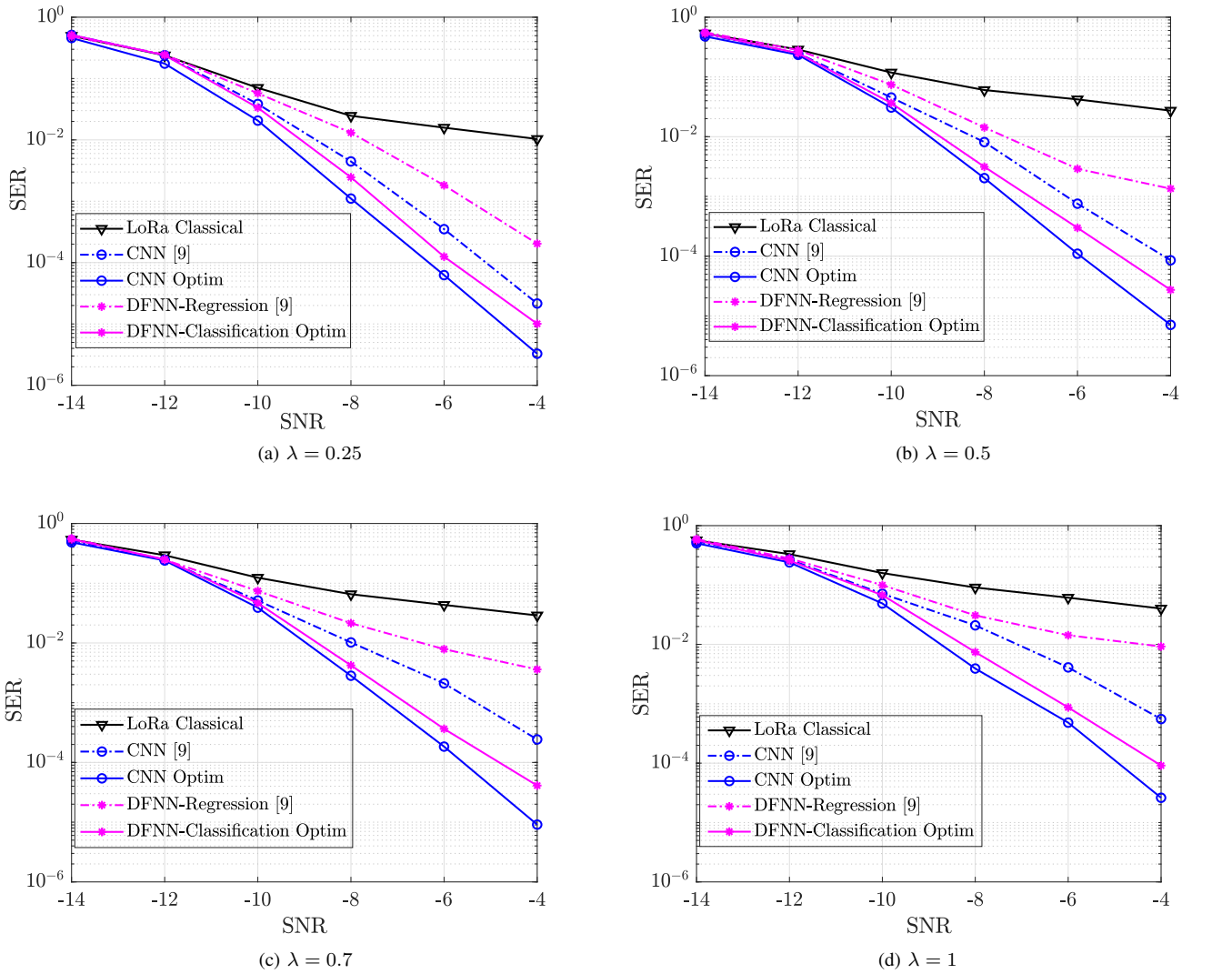

(a) $\lambda = 0.25$ (b) $\lambda = 0.5$

(c) $\lambda = 0.7$ (d) $\lambda = 1$

Fig. 7: Symbol error rate as a function of the SNR for different approaches: *classical receiver*, *DFNN-based* [9], *CNN-based* [9], and the proposed optimized DFNN and CNN-based.

REFERENCES

[1] Q. M. Qadir, "Analysis of the reliability of lora," *IEEE Communications Letters*, vol. 25, no. 3, pp. 1037–1040, 2021.

[2] A. Biral, M. Centenaro, A. Zanella, L. Vangelista, and M. Zorzi, "The challenges of m2m massive access in wireless cellular networks," *Digital Communications and Networks*, vol. 1, no. 1, pp. 1–19, 2015.

[3] B. Reynders, W. Meert, and S. Pollin, "Range and coexistence analysis of long range unlicensed communication," in *2016 23rd International Conference on Telecommunications (ICT)*, 2016, pp. 1–6.

[4] P. Edward, S. Elzeiny, M. Ashour, and T. Elshabrawy, "On the coexistence of LoRa- and Interleaved Chirp Spreading LoRa-Based modulations," in *2019 International Conference on WiMob*, 2019.

[5] A. A. Tesfay, E. P. Simon, G. Ferré, and L. Clavier, "Serial interference cancellation for improving uplink in LoRa-like networks," in *2020 IEEE 31st Annual International Symposium on PIMRC*, London, UK, 2020.

[6] P. Zhang, X. Kang, D. Wu, and R. Wang, "High-Accuracy Entity State Prediction Method Based on Deep Belief Network Toward IoT Search," *IEEE Wireless Communications Letters*, vol. 8, no. 2, pp. 492–495, 2019.

[7] J. Zhou, Y. Wang, K. Ota, and M. Dong, "AAIoT: Accelerating Artificial Intelligence in IoT Systems," *IEEE Wireless Communications Letters*, vol. 8, no. 3, pp. 825–828, 2019.

[8] Y. Yazid, I. Ez-Zazi, M. Arioua, and A. El Oualkadi, "A deep reinforcement learning approach for lora wan energy optimization," in *2021 IEEE Microwave Theory and Techniques in Wireless Communications (MTTW)*, 2021, pp. 199–204.

[9] A. A. Tesfay, E. P. Simon, S. Kharbech, and L. Clavier, "Deep learning-based signal detection for uplink in lora-like networks," in *2021 IEEE 32nd Annual International Symposium on Personal, Indoor and Mobile Radio Communications (PIMRC)*, 2021, pp. 617–621.

[10] A. A. Tesfay, E. P. Simon, I. Nevat, and L. Clavier, "Multiuser detection for downlink communication in LoRa- Like networks," *IEEE Access*, vol. 8, pp. 199 001–199 015, 2020.

[11] K. He and J. Sun, "Convolutional Neural Networks at constrained time cost," in *2015 IEEE Conference on Computer Vision and Pattern Recognition (CVPR)*, 2015, pp. 5353–5360.